Flattening and Cooling of Millimeter- and Micrometer-Sized Alumina Drops

S. Goutier, M. Vardelle, J.C. Labbe, and P. Fauchais

(Submitted May 18, 2010; in revised form September 3, 2010)

An experimental setup was developed to produce fully melted, millimeter-sized, ceramic or metallic drops with impact velocities up to 10 m/s. Such impact velocities allow achievement of impact Weber numbers, close to those of the plasma spray process ($We = 2300$) with droplets in the tens of micrometer size range. A fast camera (4000 image/s) combined with a fast pyrometer (4000 Hz), allowed the flattening of the drop to be followed. To study the flattening of micrometer-sized droplets, a direct-current (dc) plasma torch was used to melt alumina particles (around 45 μm in diameter). The experimental setup was composed of a fast (50 ns) two-color pyrometer and two fast (at best an exposure time of 2 μs) charge-coupled device cameras (one orthogonal and other tangential to the substrate). The flattening behaviors of millimeter- and micrometer-sized particles were compared. First, impacts of alumina drops (millimeter-sized) with velocities up to 10 m/s were studied. Results were then compared with micrometer-sized alumina particles (about 45 μm in diameter) sprayed with the dc plasma torch. A correlation was found between both flattening scales, and, in spite of the lower impact velocity at the millimeter scale, droplet ejections were also found as obtained at the micrometer scale. This work shows that for a sound comparison of phenomena at the two different scales it is mandatory to have Weber numbers as close as possible in both cases.

Keywords	cooling, flattening, high Weber number, micrometer splat, millimeter splat, splashing

1. Introduction

The adhesion/cohesion of plasma sprayed coatings is a key issue: A coating will never protect a substrate if it does not adhere to it! To better understand the phenomena implied, many works have been devoted to the study of a single splat formation; see the review of Chandra and Fauchais (Ref 1). This work emphasizes the difficulty of the study for plasma spraying impact of particles in a molten state with sizes between 20 and 60 μm and velocities ranging from 50 to 300 m/s with flattening and solidification times in the microsecond time range. If sophisticated pyrometers had been developed with response times of about 100 ns, the interpretation of their

S. Goutier, M. Vardelle, J.C. Labbe, and **P. Fauchais**, SPCTS Laboratory, University of Limoges, 123 Avenue Albert Thomas, 87060 Limoges Cedex, France. Contact e-mail: simon.goutier@unilim.fr and michel.vardelle@unilim.fr.

signals would still be difficult without the visualization of the flattening phenomenon. In spite of the development of fast (up to 106 frames/s) cameras, it is still impossible to follow this flattening for the same micrometer-sized particle. That is why, since the mid-1990s, many works have been devoted to the flattening of millimeter-sized metal drops (Ref 1), occurring in the millisecond time range. However most results were obtained with free-falling drops (velocities below 3 m/s), resulting in Weber numbers ($We = \rho v^2 d / \sigma$, where ρ is the liquid mass density, σ the surface tension of the drop, d the initial diameter of the particle, and v the particle impact velocity) much lower than those obtained in plasma spraying conditions. The comparison of phenomena at both scales (millimeter and micrometer size) is thus rather difficult. If for tin drops, using a centrifugal drop setup, impact velocities up to 30 m/s have been achieved (Ref 2), this material is unfortunately not sprayed by thermal processes. However this experiment shown the influence of the Weber number on the flattening process. The aim of the present work is to compare the flattening and cooling of drops and droplets of the same material. The main difficulty was to achieve imaging at the micrometer scale. To our knowledge, only one author has used a very fast camera (1 frames/μs) to follow the flattening of a single zirconia particle impacting on a cold substrate (Ref 3). Some authors have also studied the impact of metal and ceramic particles on glass or Inconel substrates at different times of the flattening process but for different particles, assumed to impact with the same parameters (Ref 4, 5). However, works devoted to the following alumina particle impacts, followed by their flattenings and splashings are not numerous. Indeed, the latent heat of fusion (L_f) and the specific heat (c_p) of

that material are high, compared with those of zirconia particles, and their melting is more difficult. Moreover, as the Planck's radiance is also lower, it is more difficult to collect the light generated by the particle at the impact. The only works published, with photos taken over a long period (250 μs), have shown many droplet ejections (Ref 6), but the questions are: When do these ejections occur and why?

According to some authors, the solidification around the edges of spreading droplets creates a solid rim that obstructs the liquid flow and triggers splashing (Ref 2). In other works, the flattening of the particle mainly depends on its wettability and solidification (Ref 7). Increasing the substrate temperature raises the wettability and so reduces splashing. Others authors suggest that the splat fragmentation is due to the presence of adsorbates and condensates on substrate surface (Ref 8) or to the substrate roughness (Ref 9).

This work is devoted first to the study of the impact of alumina drops (millimeter-sized) with impact velocities up to 10 m/s corresponding to Weber numbers similar to those achieved in real plasma spray conditions with micrometer-sized particles. A fast camera (4000 image/s) combined with a fast pyrometer (4000 Hz), allows the drop flattening to be followed.

Then the flattening at the micrometer scale was studied with a direct-current (dc) plasma torch spraying micrometer-sized alumina particles (about 45 μm in diameter). The experimental setup was composed of a fast (response time = 50 ns) two-color pyrometer and two fast (exposure time = 0.5 μs) CCD cameras (PCO sensicam, fast shutter; PCO AG, Kelheim, Germany) (one orthogonal and the other one tangential to the substrate).

2. Experimental Setup

Experiments were carried out with two experimental techniques for studying impact and flattening phenomena. The first was a modified free-falling setup to study millimeter-sized drops with high Weber numbers, and the second was a plasma spraying setup with micrometer-sized droplets.

Running these two studies in parallel enabled comparison, at spatial and time scales differing by almost three orders of magnitude, of particle flattening and cooling on smooth 304 L stainless steel substrates, preheated or not.

2.1 Study of Millimeter-Sized Particles

To produce liquid ceramic drops, an alumina rod was introduced and melted in an electrical arc furnace (Fig. 1). A suspended drop was formed. When the gravity force overcame that of the surface tension, the drop fell. The furnace is filled with argon. The substrate, fixed onto a pneumatic jack, could be moved up during particle fall and the relative impact velocity could reach up to 10 m/s (Ref 10).

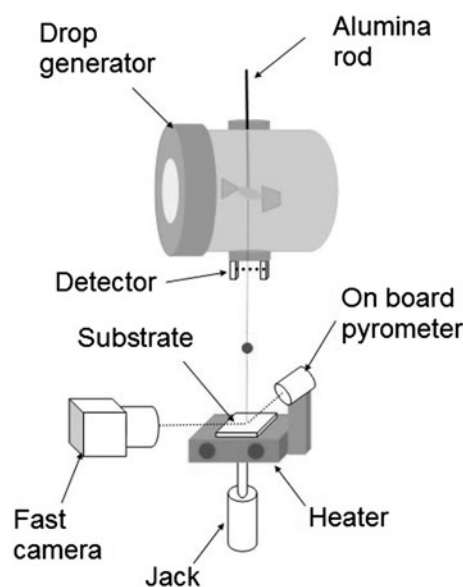A detector located at the chamber output generated a TTL pulse (5 V, 10 μs) when one single drop crossed its

Fig. 1 Drop generator and diagnostics for millimeter-sized drops

measuring volume. This pulse was then directed to the measuring system composed of a fast camera (FAST-CAM-1024PCI; Photron, Tokyo, Japan), targeting the substrate tangentially in order to follow the matter ejection during the drop flattening. Of course, in order to better determine the location of these ejections, the camera was not absolutely parallel to the substrate, but a small angle (2°) existed, which made the other edge of the splat visible. Finally, a fast two-color pyrometer measured the drop temperature at impact.

2.2 Study of Micrometer-Sized Particles

Particles were plasma sprayed using a dc plasma torch (PTF4 type) with a 6 mm internal diameter nozzle and running with a mixture of argon-hydrogen. The arc current was 650 A, the argon flow rate 33 L/min with 25 vol.% hydrogen. An alumina powder with particle sizes between 40 and 50 μm was used in this study. These spray conditions resulted in fully melted particles with velocities at impact around 200 m/s. Splats were collected on a smooth ($R_a = 0.06$ μm) stainless steel 304 L substrate positioned 110 mm downstream of the nozzle exit (Fig. 2).

Three shieldings were used to select particle trajectories close to the plasma axis. The first one was a mobile water-cooled shield (hole of 5 mm), which was fixed 70 mm downstream of the torch nozzle exit. The second one (hole of 1.5 mm) was disposed at 80 mm, the last one, with a hole of 600 μm, and fixed at 90 mm.

The measuring system was composed of:

- Measurement of in-flight droplet velocity by a 2-point measuring optical detector and temperature by a fast (response time = 50 ns) bichromatic pyrometer following the particle temperature during flattening and then cooling. The two wavelengths of the bichromatic pyrometer are 690 and 710 μm, respectively.
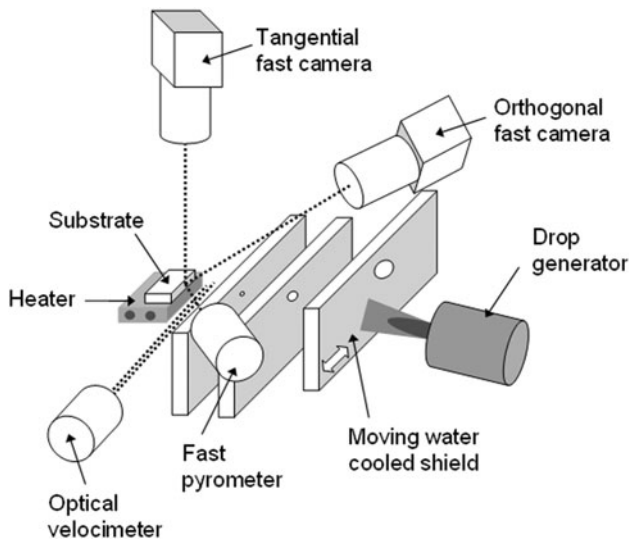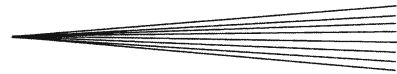
Fig. 2 Experimental setup and diagnostics to follow the impact of a single alumina particle at the micrometer scale

- Imaging techniques, which allowed following the flattening of the particle. A macro lens with a focal distance of 200 mm and two focal doublers was fixed on each camera. The main advantage of such lenses, compared with a long-distance microscope (Questar type), is that the collected light is more important. One camera was set orthogonal to the substrate and other one was tangential to it.

With different exposures times and a variable time delay relative to the impact time, it was possible to observe the flattening at different times, but for different particles (assuming they all had the same parameters at impact).

2.3 Substrate

Substrates were made of stainless steel (304 L) and were mirror polished using SiC paper 4000. They were fixed on copper supports heated up to 200 °C with a heating rate of 0.5 °C/s by two small resistances (each one with a power of 150 W). A monochromatic pyrometer (Modline 5, 5 μm, 10 ms of response time; IRCON, Santa Cruz, CA) controlled the substrate temperature during the preheating stage. The substrate was disposed 110 mm downstream of the nozzle exit.

3. Results

3.1 Millimeter-Sized Drops on Smooth Substrates

Figure 3 presents tangential pictures, taken at different times, of the flattening on a cold stainless steel substrate ($T_{substrat} = 20$ °C) of an alumina drop 5 mm in diameter. Figure 4 shows a hot preheated substrate ($T_{substrate} = 200$ °C).
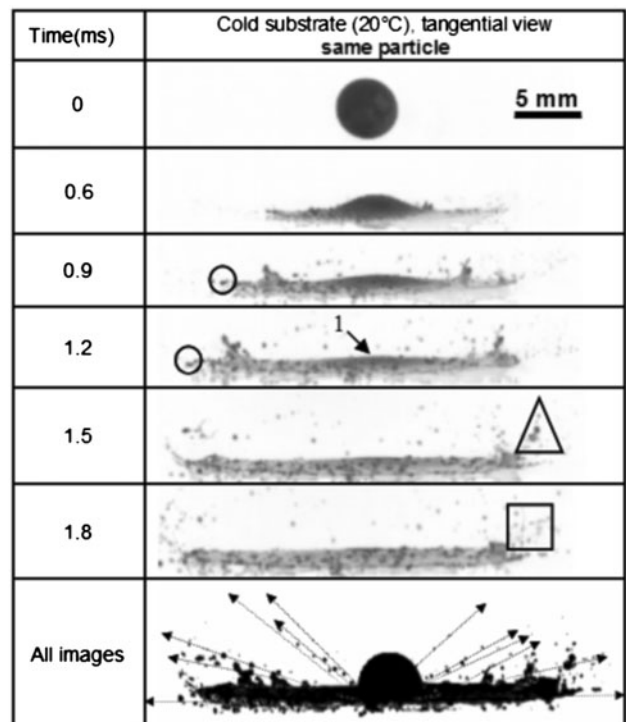

Fig. 3 Tangential view of a single alumina drop impacting on a cold stainless steel substrate (20 °C), arrow 1 shows the position of the rear edge, all images have the same scale
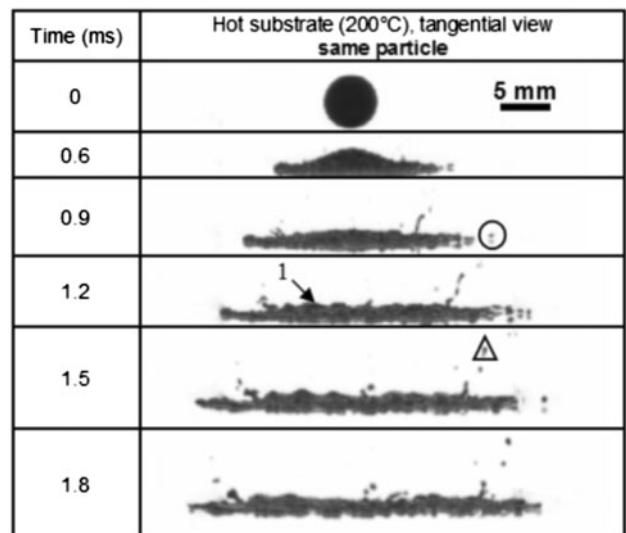

Fig. 4 Tangential view of a single alumina drop impacting on a hot stainless steel substrate (200 °C), arrow 1 shows the position of the rear edge, all images have the same scale

On a cold surface, it can be seen that the splashing phenomenon consisted of:

- A parallel ejection issued from splat edges with a velocity below 50 m/s, (circled particles at 0.9 and 1.2 ms).

- An angular ejection also from splat edges with a mean velocity of 10 m/s (triangle droplets at 1.5 ms), ejections located on the rear edge (arrow 1 in Fig. 3 at 1.2 ms) and not in the splat.
- A cloud ejection (squared droplets at 1.8 ms).

When all images were superposed (see last row called "all images"), the different trajectories appeared more clearly, and some wave matter propagation could be seen; these waves generated more important angular ejections. In parallel to these waves, some ejections appeared near the impact center (between 0.6 and 0.9 ms).

On a hot substrate (200 °C), only few ejections with weak velocities (lower 8 m/s) were observed, but parallel ejections (circled in Fig. 4 at 0.9 ms) and angular ones (triangled in Fig. 4 at 1.5 ms) were present. The cloud ejection was not visible on a hot substrate. No matter which wave was observed, the few angular ejections coming from expanding matter film also appeared between 0.6 and 0.9 ms. Finally, the type of ejection found on a hot substrate was similar to that obtained on a cold one, but the amplitude of phenomena was drastically reduced.

3.2 Effect of Wet Substrate on the Flattening of a Millimeter-Sized Particle

For a better understanding of the desorption phenomena when a particle impacted on cold substrate, a thin water film was laid on the substrate. The water droplets on the substrate had a mean diameter of 300 μm (±50 μm). Figure 5 presents the impact of an alumina droplet on a wet and cold substrate. At $t = 0$ s, the small droplets were visible on the substrate (see Fig. 5, arrow 1 at $t = 0$ s). The maximum flattening diameter was reached in about 4 ms. At that time, a lot of flowing matter was concentrated at the splat edges and induced some ejections. Some instabilities appeared in the thin film between the splat center and splat edges (see arrow 2, Fig. 5 at $t = 4$ ms). These

instabilities induced some holes into the film (see arrow 3, Fig. 5 at $t = 4.2$ ms) and breaks of the thin matter film by a dewettability phenomenon. Finally, no splat was obtained.

3.3 Comparison Between Hot and Cold Substrates for Micrometer-Sized Particles

Figure 6 presents the impact of an alumina particle on a stainless steel for different substrate temperatures. The first and the second rows show, respectively, the pictures focused orthogonally to the substrate and those focused tangentially. The exposure time of the first camera was 10 μs; the acquisition started at impact. For the second camera, the exposure times were sequenced over 10 μs (open 0.5 μs, closed 0.5 μs), and the acquisition started 1.8 μs before impact in order to validate the velocity and had an estimation of the particle diameter. In the last row, the view of the final splat is presented. Comparison of both cases (cold and hot substrate) shows the mean differences are the drop splashing on the substrate.

Indeed, for a cold surface it seems that the particle was completely destroyed at impact; the shape of the resultant splat was a circle around the impact center with a radius of 186 μm. In the photo from camera 1, it can be seen that splashing took place at the splat edges at about a distance of 200 μm from the splat center. So the matter circled around the impact center corresponded to the maximum flattening of the particle and probably to the ejection area. Many ejections can be seen in the photo from camera 2. Some were parallel to the substrate, and others were at angle to it.

On a hot surface (heating 8 min at 200 °C), no splashing was observed and the resulting splats were disk shaped. For another heating period (heating 16 min at 200 °C), the splat was no longer disk shaped and some matter ejection occurred during the flattening, but most of the splat remained on the substrate. Near the impact center in the photos from camera 2, some ejections with an angle of 45° can be observed.
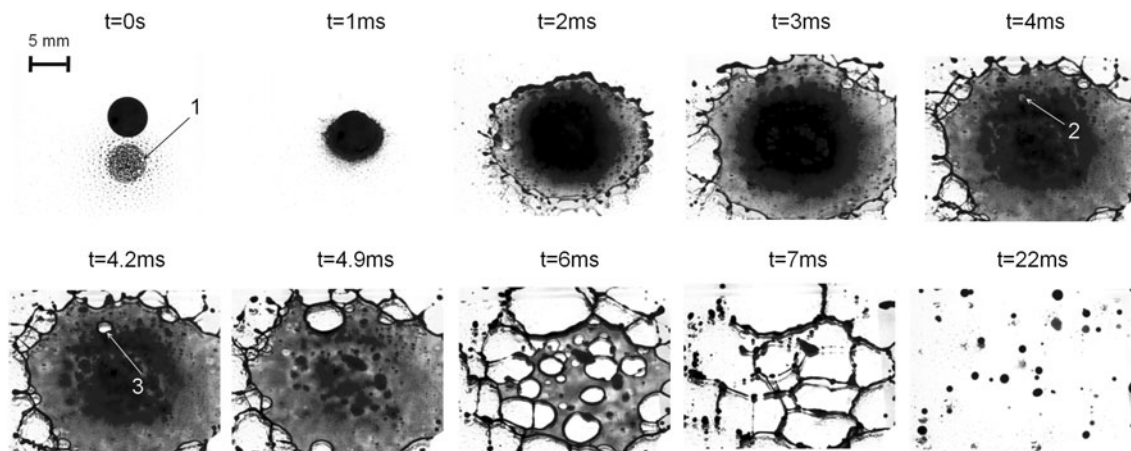

Fig. 5 45° view of a single alumina drop impacting on a wet and cold stainless steel substrate (20 °C), all images have the same scale
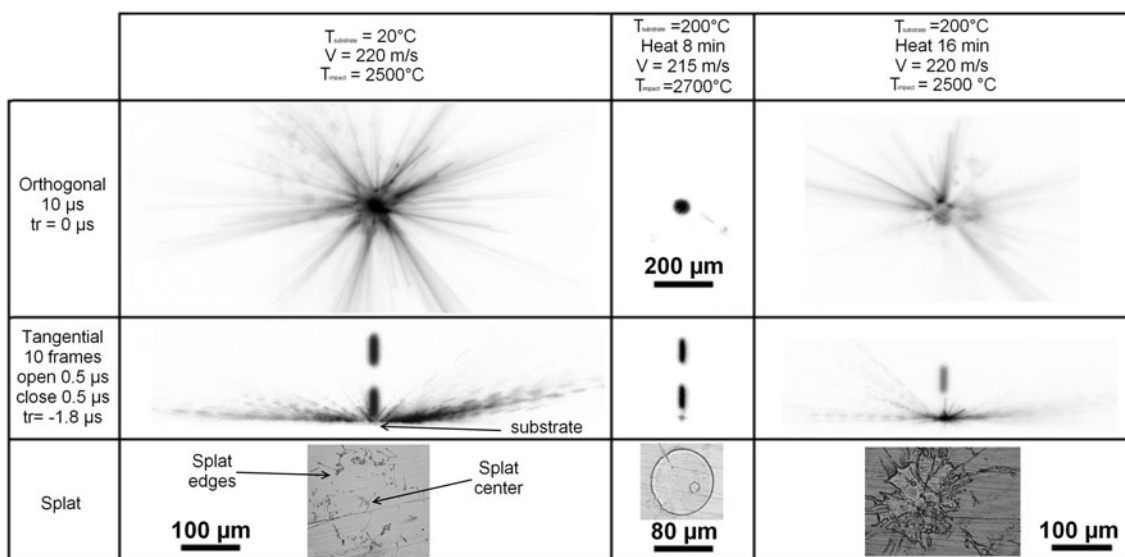
Fig. 6 Comparison between cold and hot substrates and for different preheating times. First row: droplet and substrate parameters, second and the third rows: pictures of the perpendicular camera and that of the tangential one, last row: microscopic view of the resulting splat, t_r: time corresponding to the delay at impact for the camera triggering, all flattening images have the same scale

The question is: when splats are disk shaped do any ejections occur at the splat edges? In order to answer that question and for a better understanding of the splashing phenomenon, the pyrometer signals must be analyzed.

Figure 7(a) presents pyrometer signals (triggered at impact) at two wavelengths (λ_1, λ_2) and the calculated corresponding bichromatic temperature $[T = f(t)]$ for the case of a cold surface. The case of a hot surface is presented in Fig. 7(b) and (c).

The first conclusion is that when the splat was disk shaped the pyrometer signal decreased very quickly compared with the case where splashing existed (cold surface and hot surface heated during 16 min). On a cold surface, the maximum signal (at the wavelength λ_1) was 35 a.u., and it was reached in 1 μs, and the slope, corresponding to the flattening stage, was 35 a.u./μs. On a hot surface (heated during 8 min), the slope was only 25 u.a./μs. For the case of heating for 16 min, the slope was 27 u.a., rather close to that of the previous case. So there was no clear difference between both preheating temperatures. At the same temperature, the signal intensity mainly depended on the emitting surface of the flattening particle. So, on a cold surface the flattening was faster than on a hot one.

When the three bichromatic temperature evolutions were compared, the cooling on a hot surface was faster than that on a cold surface. Indeed, on a cold substrate, the cooling rate was about 110 °C/μs, while on a hot substrate preheated for 8 min at 200 °C the cooling rate was about 900 °C/μs and for the surface preheating for 16 min at 200 °C, the cooling rate was about 300 °C/μs. On temperature curves at approximately 2100 °C, the three curves present a plateau, preceded by a slight decrease. It can be attributed to a solidification plateau

preceded by an undercooling phenomenon. When considering the impact on the same substrate at different preheating times with the same heating temperature, the cooling was not similar.

In order to understand better the splashing, it is necessary to achieve a reproducible phenomenon. Unfortunately the splashing study on the hot surface was not very easy, because of difficulties in controlling the surface roughness and oxide composition and thickness; thus more work is necessary. Section 3.4 presents only splashing on cold surfaces.

3.4 Splashing Phenomena of a Micrometer-Sized Particle Impacting on a Cold Surface

Figure 8 presents different images captured at different moments of the flattening stage. The reference time ($t = 0$) corresponded to the particle impact. For that, the pyrometer was triggered at the particle impact while cameras were triggered at different times of the particle flattening time, with positive or negative delays noted t_r. The exposure times of both cameras were 2 μs, and in Fig. 8 shows (see the first column) both camera images and correspondingly shaded areas on the thermal signal given by the bichromatic pyrometer. For easier understanding, only the signal at wavelength λ_1 is shown. The images at different flattening times were obtained for different particles (see second and third columns called, respectively, camera 1 and camera 2). Of course, only particles with the same impact velocity (± 10 m/s) and in-flight temperature (± 100 °C) were considered.

In the first row of the table, corresponding to a camera triggering $t_r = -1.8$ μs, it can be seen that there was no ejection at impact and so no impact splashing. In the next row, corresponding to a camera triggering $t_r = -1.2$ μs, the
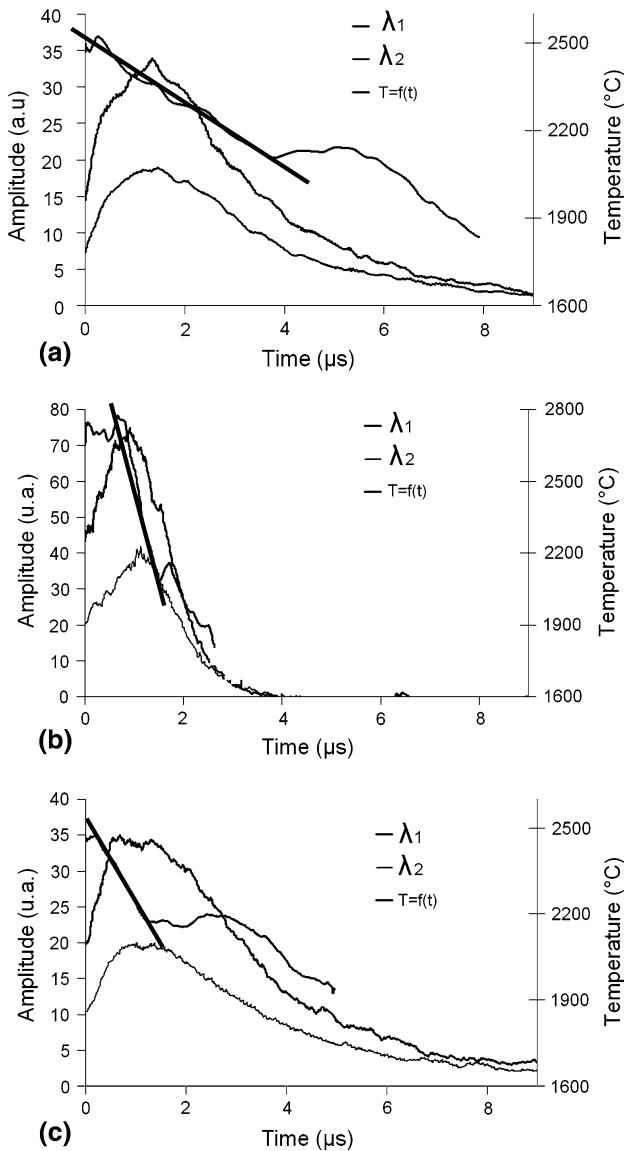
Fig. 7 Different calculated temperatures $[T = f(t)]$ for the pyrometer signals at two wavelengths $(\lambda_1, 2)$, for (a) cold surface (20 °C), (b) hot surface (200 °C, heated 8 min), (c) hot surface (200 °C, heated 16 min)

camera exposure time ended at the maximum drop flattening and very few ejections occurred at the splat edges.

The next images $t_r = 0.2$ μs, correspond to the flattening stage and the beginning of the pyrometer signal decrease. In this area, the splat presented more droplet ejections and were not homogenous: splat edges and central part were more luminous than the area between them.

In the next image $t_r = 1.8$ μs, corresponding only to the pyrometer signal decrease, splat edges and central part were still luminous, but a lot of matter was ejected. These ejections were mainly parallel to the substrate (angle below 5°), and they took place at different locations of splat edges. The tangential view must be interpreted with care. Indeed, ejections indicated with the arrow (Fig. 8, row 4) are in the direction parallel to the substrate. However,

their angles seemed to be larger because their trajectories corresponded approximately to the camera axis, ejections being thus defocalized. So, on the tangential view only ejections with a trajectory in the same plane as that targeted by the camera were considered. For a longer time delay, ejections occurred in all directions and not only at the splat edges (Fig. 8, rows 5 and 6), and there are very few parallel ejections. All these phenomena probably led to the complete destruction of the splat.

4. Discussion

When the micrometer and millimeter results are compared, there is a good correlation between both flattenings. Indeed in previous work (Ref 10) on the millimeter alumina drops, it was shown that when an alumina particle impacts on a cold stainless steel substrate, the splat quickly develops a very thin film expanding around its central part, and some matter accumulates at the splat edges (see Fig. 9). Next, this matter is ejected into small droplets. Finally, the thin film is broken into solid ships and only the splat center remains on the substrate. On a hot substrate, some ejections exists but no thin film expanded around the splat center (see Fig. 9).

In this paper, the tangential view shows the presence of both ejection directions, those almost parallel to the substrate and those with an angle. The parallel ejections have higher velocities than the angular ones. Finally, the diameter of the ejected particle is reduced and a cloud of small particles is obtained. When the substrate is heated, the cloud ejection is not present.

The parallel ejection may be due to ejections at the external part of splat edges that increase with the propagation velocity of the liquid matter on the substrate. Indeed on a hot substrate, the thermal contact is better, resulting in solidification at the splat/substrate interface. Thus the flattening velocity of the matter at the flattening particle surface is reduced (Ref 11), diminishing parallel ejection.

The parallel ejections might be due to the presence of flow obstructions at the flattening particle surface, and so a matter wave is rapidly created, resulting in angular droplet ejections when this wave reaches splat edges. However, it should be noted that these waves concern only some parts of the splat and there is no ring of ejections around the splat. In some cases, the birth of these waves is linked to the generation of small droplets that are ejected. The presence of a solid rim obstructing the flow and triggering splashing is described by Dhiman and Chandra (Ref 2).

The smaller diameters of the ejected particles at the end of the flattening are probably linked to the decrease of the flattening velocity due to the splat cooling.

However a question is still raised: What is the influence of adsorbates and condensates on the splashing?

On a cold substrate, there is a lot of adsorbates/condensates (Ref 8). The experimentation with millimeter-sized particles shows that the presence of water added on
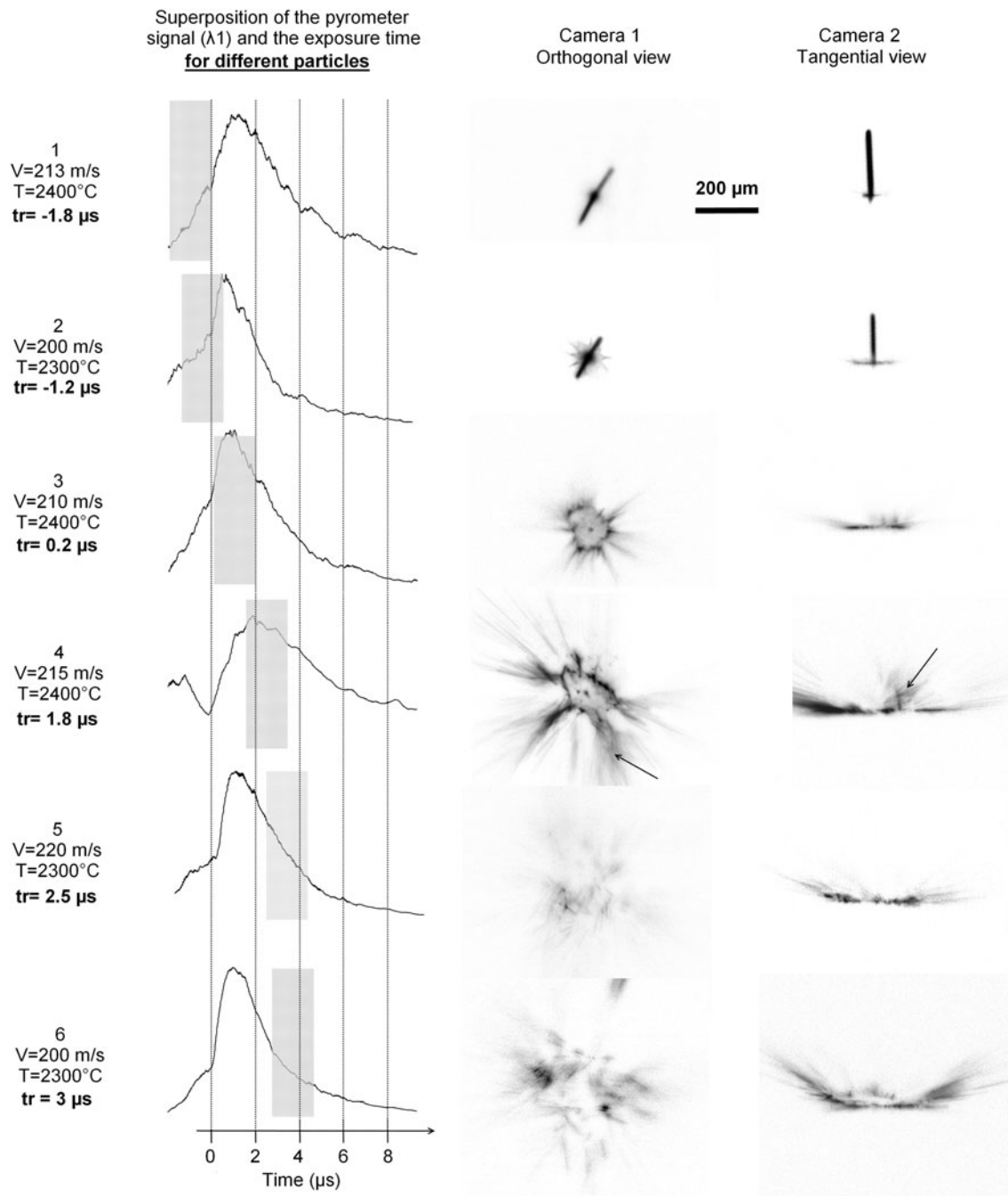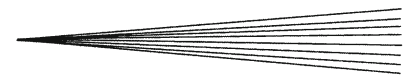
Fig. 8 Impact, on a cold stainless steel substrate, of different micrometer sized alumina particles, but with about the same velocity, the same diameter, and the same temperature at impact. The shaded area on the pyrometer signal represents the opening time of the camera shutter; all images have the same scale

the surface does not induce more splashing at splat edges than on a dry surface; only the maximum flattening diameter is modified. The vaporization of the water takes place only at the end of the flattening, and its main role is the destabilization of the liquid alumina film inducing the film breakage.

On a hot substrate, adsorbates/condensates are not present (Ref 11), and, if the splashing exists, the central part of the splat is not destroyed; only its edges are concerned. Splashing is not visible when the cooling time is very short (less than 1 μs to reach the solidification plateau).

The main role of adsorbates/condensates is to increase the flattening by reducing the contact with the substrate, flattening followed by breakage of the thin film expanding around the central part of the splat.
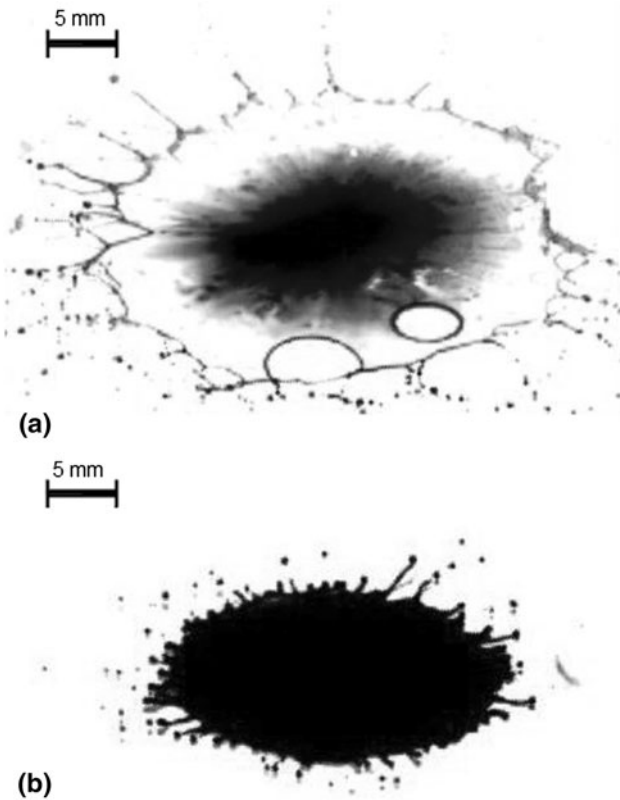
Fig. 9 Alumina drop (5 mm in diameter) flattening on polished stainless steel, 1.6 ms after impact, for two different substrate temperatures at the same Weber number ($We = 2300$). (a) Cold substrate (20 °C). (b) Hot substrate (400 °C) (Ref 10)

The splashing of the flattening drop is mainly related to the splat cooling and so indirectly to the presence of adsorbates.

A question is still pending: What are the reasons of the cooling rate modification between both hot substrates heating times? Without detailed analyses of the substrate surface, it is difficult to answer that question. Indeed some authors have shown that the splat shape is strongly linked to the substrate surface chemistry (Ref 12-14) and to the substrate roughness (Ref 15). So, for future work, the modification of the particle splashing will be studied in parallel with the evolutions of the substrate chemistry and roughness.

5. Conclusion

A good correlation has been found between millimeter- and micrometer-sized particles, impacting, flattening, and solidifying onto smooth 304 L stainless steel substrates preheated or not, in spite of the slightly lower Weber numbers obtained at the millimeter scale. These preliminary results have shown that it is necessary to achieve higher Weber numbers than those resulting from free falling for millimeter-sized particles to obtain a better comparison of phenomena at both scales.

On a cold surface, parallel and angular ejections are observed. Droplets ejected almost parallel to the substrate are faster than those ejected at an angle. The main angular ejections result from the propagation of localized waves on the flattening particle surface. When these waves are generated, there are some ejections with an angle higher than those of other ejections. These waves are probably generated when irregularities are present at the surface on which the liquid is flattening. The breakage of the thin liquid film expanding around the splat center could be attributed, among others assumptions, to the vaporization of adsorbates and condensates present at the substrate surface.

On a hot surface, the types of ejections are similar to those obtained on a cold one, but the quantity of droplet ejections is drastically reduced. Also no splat center destruction is observed, confirming the role of adsorbates and condensates on the rupture of the thin expanding film. In some cases, when the cooling rates are very fast no splashing is visible and a disk-shaped splat is obtained. So the existence of a link between the cooling time and the presence of splashing at the splat edges is not at all improbable. However, on hot surfaces more studies are necessary to determine precisely, as a function of the preheating procedure, the composition and topography of the oxide layer present at the substrate surface.

References

1. S. Chandra and P. Fauchais, Formation of Solid Splats During Thermal Spray Deposition, *J. Thermal Spray Technol.*, 2009, **18**(2), p 148-180
2. R. Dhiman and S. Chandra, Freezing-Induced Splashing During Impact of Molten Metal Droplets with High Weber Numbers, *Int. J. Heat Mass Transf.*, 2005, **48**, p 5625-5638
3. K. Shinoda, H. Murakami, S. Kuroda, S. Oki, K. Takehara, and T.G. Etoh, High-Speed Thermal Imaging of Yttria-Stabilized Zirconia Droplets Impinging on a Substrate in Plasma Spraying, *Appl. Phys. Lett.*, 2007, **90**, p 194103/1-194103/3
4. A. McDonald, S. Chandra, and C. Moreau, Photographing Impact of Plasma Sprayed Particles on Rough Substrates, *J. Mater. Sci.*, 2008, **43**, p 4631-4643
5. A. McDonald, S. Chandra, M. Lamontagne, and C. Moreau, Photographing Impact of Plasma-Sprayed Particles on Metal Substrates, *J. Thermal Spray Technol.*, 2006, **14**(4), p 708-716
6. C. Escure, M. Vardelle, and P. Fauchais, Experimental and Theoretical Study of the Impact of Alumina Droplet on Cold and Hot Substrates, *Plasma. Chem. Plasma Process.*, 2003, **23**(2), p 185-221
7. Y. Tanaka and M. Fukumoto, Investigation of Dominating Factors on Flattening Behaviour of Plasma Sprayed Ceramic Particles, *Surf. Coat. Technol.*, 1999, **120-121**, p 124-130
8. X. Jiang, Y. Wan, H. Herman, and S. Sampath, Role of Condensates and Adsorbates on Substrate Surface on Fragmentation of Impinging Molten Droplets During Thermal Spray, *Thin Solid Films*, 2001, **385**, p 132-141
9. M. Raessi, J. Mostaghimi, and M. Bussmann, Effect of Surface Roughness on Splat Shapes in the Plasma Spray Coating Process, *Thin Solid Films*, 2006, **506-507**, p 133-135
10. S. Goutier, M. Vardelle, J.C. Labbe, and P. Fauchais, Alumina Splat Investigation: Visualization of Impact and Splat/Substrate Interface for Millimeter-Sized Drops, *J. Thermal Spray Technol.*, 2010, **19**(1), p 49-55
11. M. Fukumoto, E. Nishioka, and T. Nishiyama, New Criterion for Splashing in Flattening of Thermal Sprayed Particles onto Flat Substrate Surface, *Surf. Coat. Technol.*, 2002, **161**, p 103-110
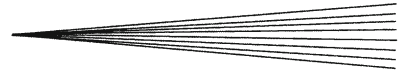
12. S. Brossard, P.R. Munroe, A.T.T. Tran, and M.M. Hyland, Study of the Microstructure of NiCr Splats Plasma Sprayed on to Stainless Steel Substrates by TEM, *Surf. Coat. Technol.*, 2009, **204**, p 1608-1615
13. A.T.T. Tran, M.M. Hyland, T. Qiu, B. Withy, and B.J. James, Effects of Surface Chemistry on Splat Formation During Plasma Spraying, *J. Thermal Spray Technol.*, 2008, **17**, p 637-657
14. A. McDonald, C. Moreau, and S. Chandra, Effect of Substrate Oxidation on Spreading of Plasma-Sprayed Nickel on Stainless Steel Substrate, *Surf. Coat. Technol.*, 2007, **202**, p 23-33
15. J. Cedelle, M. Vardelle, and P. Fauchais, Influence of Stainless Steel Substrate Preheating on Surface Topography and on Millimeter- and Micrometer-Sized Splat Formation, *Surf. Coat. Technol.*, 2006, **201**(3-4), p 1373-1382

Peer Reviewed